CFD and Finite Element Investigation of Water Impact on Composite Panels

Nuno Rodrigo Soares Borges e Silva
Instituto Superior Técnico, Universidade de Lisboa, Lisbon, Portugal

ABSTRACT: In this study, the effects of the water impact induced loads, also known as slamming loads, on sandwich composite structures are studied. This fluid-structure interaction problem is investigated using the ALE formulation included in the commercial software LS-DYNA. The computational fluid dynamics model presented is validated through the comparison of the rigid structure results with published experimental data. The finite element analysis is also validated through the simulation with input data given from another published research and with the comparison of the composite structural results from the same research. The water entries of composite panels with the combination of different deadrise angles and entry velocities are simulated. The results of the slamming loads and displacements on the panel are then summarized and discussed.

Keywords: Slamming composite plate, FSI plate slamming, ALE formulation

1 INTRODUCTION

In naval architecture, "slamming" is the term used to describe the impact of the ship hull onto the water surface at high velocity. The impulsive loads due to slamming can be very extreme, not only on the bottom of the ship but also in the upper regions of the hull where there is a lot of water displacement and splash up. The earlier studies have concluded that the deadrise and the impact velocity are the parameters that contribute the most for this type of hydrodynamic loading on the structure. Generally, the slamming pressure is higher when the velocity is higher and the deadrise is lower. Most researchers applied the simplified approach to the hull slamming problem by considering a rigid body for calculating the hydrodynamic loading and then projecting its structural response onto the flexible structure in quasi-static manner.

The local hydroelastic effect on slamming problems has been paid much attention since 1990s , due to the development of high-speed vessels. Faltinsen (1999) showed that the significance of hydroelasticity for the local slamming-induced maximum stresses increased with the decreasing of the deadrise angle and the increasing of the impact velocity. A review work of the slamming of ships has been presented by Wang and Guedes Soares (2017). It has been concluded that the global hydroelastic response of ship hulls is of importance for long and slender ships, including the recent ultra large containerships. For shorter ships this can only occur if they are made of composite materials, which are significantly more flexible than steel (Santos et al., 2009; Qin and Batra, 2009).

Nowadays, the use of composite materials in the marine industry is increasing, because of the excellent strength to weight characteristics, corrosion resistance, and lower maintenance and repair costs. Marine composites also have significant drawbacks, such as lower impact resistance and lower quasi-isotropic elastic modulus. It's very important to take special care with the slamming loads that may be induced to these ship's structures as these vessels also have the tendency to be designed with small deadrise angles and to reach high speeds, which as explained earlier, results in very high slamming loads.

Being the composite materials composed by at least two materials, it imposes additional difficulty when designing structures with this type of materials. The added difficulty on the design is due to the fact that these materials have very different properties and although the resin can be considered isotropic, the fibres are generally orthotropic. Using a CFD method for calculating the loadings on the structure in conjunction with FEM for analyzing the actual structural response is one of the fastest, safest and cheaper ways of designing composite structures that are subjected to hydrodynamic loads. The coupled CFD/FEM methods have been widely used to investigate the slamming problem of ships. Lu et al. (2000) employed the coupled BEM/FEM to study the hydroelastic effects with the panel modelled as a Timoshenko beam. The fully coupled ALE/FEM has been used by Wang and Guedes Soares (2014, 2016)

to investigate the hydroelastic water entry of an elastic wedge section and a flat steel plate.

In this study, the water entry of a composite panel is simulated using the coupled ALE/FEM method which is implemented in LS-DYNA. The ALE method is validated through the comparisons of slamming loads with the published experimental data considering both a rigid and a flexible composite panel. The hydroelasticity effect in the water entry of wedges is studied through the comparison of the results obtained for the rigid wedge with the ones obtained for the flexible composite wedge. Different deadrise and entry velocities are applied.

2 THEORETICAL BACKGROUND

The slamming problem has been in investigation for a long time and although the current tendency is to approach these problems using numerical methods, the slamming problem was firstly approached using some of the analytical and experimental methodologies explained in this chapter.

2.1 *Slamming formulations*

The slamming problem was firstly theoretically presented by von Karman (1929) who estimated the water impact forces on the sea plane floats by using the momentum theory. Later, Wagner (1932) presented an asymptotic solution for the water impact of 2D rigid bodies with small deadrise. This theory is proposed with the assumptions that the fluid is ideal, the gravity acceleration can be neglected and that the wedge draft during the water entry is much smaller than the wetted width. Figure 1 presents the water entry problem of a wedge section, where V is the entry velocity, β the deadrise angle and L the half-wetted width:

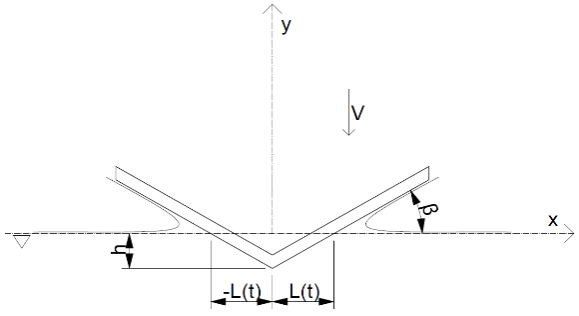

Figure 1. Water entry problem of a wedge section.

Wagner (1932) defines the velocity potential as:

$$\emptyset = -V^2\sqrt{L^2 - x^2}, |x| \leq L(t) \quad (1)$$

The pressure distribution is given by the Bernoulli equation. Neglecting its gravity term results in:

$$\frac{p-p_0}{\rho} = -\frac{d\emptyset}{dt} - \frac{1}{2}\left(\left(\frac{d\emptyset}{dx}\right)^2 + \left(\frac{d\emptyset}{dy}\right)^2\right) \quad (2)$$

The wetted width is given by:

$$L(t) = \frac{\pi}{2\tan\beta}\int_0^t V(t)\,dt \quad (3)$$

and the slamming pressure coefficient is defined as:

$$C_p = \frac{p-p_0}{\frac{1}{2}\rho V^2} \quad (4)$$

Substituting equations (1) (3) and (4) in the Bernoulli equation and assuming that the impact velocity is constant, yields:

$$C_p = \frac{\pi}{2\tan\beta}\frac{L}{\sqrt{L^2-x^2}} - \frac{x^2}{L^2-x^2} \quad (5)$$

Which is then solved for the maximum slamming pressure coefficient of Wagner's theory:

$$C_{p\,max} = 1 + \frac{\pi^2}{4\tan^2\beta} \quad (6)$$

Based on experimental tests, Ochi and Motter (1973) presented the non-dimensional pressure coefficient in a form of a proportional constant:

$$k = \exp(1.377 + 2.419a_1 - 0.873a_3 + 9.624a_5) \quad (7)$$

where a_1, a_3, a_5 are the regression coefficients, that model the section. Stavovy and Chuang (1976) also presented a regression polynomial for the non-dimensional coefficient:

$$k = \frac{288k_1}{\cos^4\beta(x,t)} \quad (8)$$

where k_1 is a coefficient that is dependent on the deadrise and can be obtained from the polynomials presented in the same research.

2.2 *Composite material formulations*

The most common type of composite material used in the marine industry is the FRP, that is composed by a resin, which is the matrix, and the fibres, which are the reinforcement material. The sandwich construction is another type of FRP application, in which, instead of building a solid laminate, a lighter material is used to quickly build thickness with small weight increment. The laminate will be composed of two FRP skins with a core material in the middle, usually a foam or a honeycomb. As the core material is much lighter than the skins, its thickness can be very high when compared with the skins. This will result in a very stiff and light composite. Since the skins are situated at the outer part of the laminate and are much stronger and stiffer than the core material, all the tensile and compressive loads are absorbed by them. Then, the core material will

mainly be subjected to shear stresses induced from the skins and eventually some compressive stresses.

When working with FRP composite materials, one of the most important factors that influences the final composite properties is the ratio between the fibres and the resin. This ratio can be expressed in terms of weight or volume and can be presented in relation to the resin or to the fibre.

The following expressions show the relations between the ratios, the volumes and the masses in the composite, where m, v, ρ is the mass, volume and density, respectively, M is the mass fraction and V is the volume fraction. The f and r index will indicate whether the property its related to the fibre or to the resin:

$$M_f = \frac{m_f}{m_f + m_r} \tag{9}$$

$$V_f = \frac{v_f}{v_f + v_r} \tag{10}$$

The general expressions for the density appear as:

$$\rho_f = \frac{m_f}{v_f} \tag{11}$$

$$\rho_r = \frac{m_r}{v_r} \tag{12}$$

Relating these expressions, results in:

$$M_f = \frac{\rho_f V_f}{\rho_r + V_f(\rho_f - \rho_m)} \tag{13}$$

$$V_f = \frac{1}{1 + \frac{\rho_f}{\rho_r}\left(\frac{1}{M_f} - 1\right)} \tag{14}$$

For composite materials, the thickness, in mm, of one cured ply can be approximated by:

$$t_{ply} = \frac{m_f}{\rho_f * V_f * 1000} \tag{15}$$

Relating the thickness with the fiber mass fraction results in:

$$t_{ply} = \frac{m_f * \left(\frac{1}{\rho_f} + \frac{1 - M_f}{M_f * \rho_r}\right)}{1000} \tag{16}$$

In a production environment, it becomes easier to use equation (16) instead of (15), as the fibre mass fraction can be easily calculated at the production facility by the expression (9), since both the weight of the fibres before the lamination and the final part weight can be easily determined.

3 COMPUTATIONAL MODEL

The water entry problem is simulated by using the ALE algorithm which is implemented in LS-DYNA 971, an explicit finite element commercial code. The calculations are performed by using the double precision solver. A multi-material Eulerian formulation and the penalty coupling algorithm developed by Aquelet et al. (2005) are applied to simulate the fluid and structure interaction problem. The Lagrangian formulation is used to describe the plane-strain deformations of the structure with considered geometric nonlinearities.

3.1 *Materials*

The composite wedge modeled in this study is made from a sandwich laminate. The laminate schedule is composed by three layers of 800 g/m^2 glass woven roving (0º/90º) at each skin being the layers oriented along and perpendicular to the wedge. The core material selected is a PVC foam with a density of 80 kg/m^3 and with a thickness of 15 mm. The matrix for this laminate will be a vinylester resin. Assuming that the composite was produced using the infusion technique, the Bureau Veritas (2012) rules suggest that a mass fraction of 0.6 can be considered. With this assumption it's now possible to calculate several laminate properties using the composite material formulations proposed in the same rules. The rules also suggest that the density of E-glass type fibers can be approximated to 2.570 g/cm^3. The same goes for a vinylester resin, with a density of 1.100 g/cm^3. The total mass per square meters of dry reinforcements at each skin is 2.4 kg/m^2. Using the composite material formulations proposed by Bureau Veritas (2012), it's possible to obtain material characteristics presented in Table 1 and 2:

Table 1. Core mechanical properties.

Density	80	kg/m3
Elastic Modulus	67	MPa
Shear Modulus	31	MPa
Poisson Coefficient	0.08	-

Table 2. FRP skin mechanical properties.

Density	1675	kg/m3
Elastic Modulus (X direction)	18.31	GPa
Elastic Modulus (Y direction)	18.31	GPa
Elastic Modulus (Z direction)	5.83	GPa
Shear Modulus (X direction)	2.65	GPa
Shear Modulus (Y direction)	2.65	GPa
Shear Modulus (Z direction)	2.38	GPa
Poisson Coefficient (XY direction)	0.072	-
Poisson Coefficient (XZ direction)	0.226	-
Poisson Coefficient (YZ direction)	0.226	-

3.2 *Model geometry*

The two-dimension computational model, presented in Figure 2, is composed by the air, the water and the wedge. As suggested by Luo et al. (2011), the water domain dimensions should be at least five times the dimensions of the wedge, in both x and y directions. Since the wedge must be initially modeled above the air-water interface, the air domain height must be able to contain the wedge body with sufficient margin around the body. The air domain width should also be equal to the water domain. Since the problem is symmetric, only half of the wedge, air and water is modeled. The water and air sizes are fixed, being the water domain size 1250x700mm and the air domain size 1250x200mm. The wedge length is fixed at 300mm, being the deadrise angle varied according to the simulation. The wedge's keel point is initially situated 25mm above water.

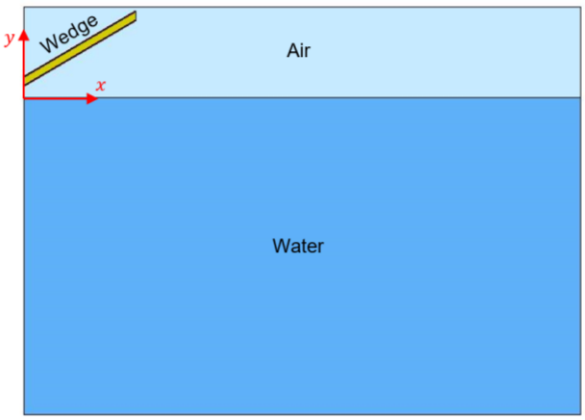

Figure 2. Model geometry.

3.3 *Element selection*

To model the fluid, the elements modeling the water and the air must be ALE solid elements, which is an eight-node brick element. The composite wedge mesh can be modeled either using only shell elements, only solid elements or a combination of both. Modeling the wedge mesh using only shell elements can result in a simpler model. Composite parts are often modeled using shell elements as they generally approximate well the "sheet" behavior (thickness much smaller than length and width). As the object in study is composed by a composite sandwich structure, it could make sense to model at least the core material with solid elements, as the thickness of this material is higher. Despite the added difficulty to get plausible values for the composite materials (especially in the out of plane direction) it was decided to model the whole wedge mesh in solid elements, also eight node structural bricks. This enables to obtain structural results in the out of plane direction which is along the thickness of the structure. This can be useful to address structural problems like delamination or core failure due to excessive compression stresses.

3.4 *Mesh*

The mesh presented in Figure 3 is similar to the one presented in Luo et al. (2011) research, in which is suggested that the water domain in which the wedge is expected to penetrate must be refined. This refinement is performed equal in both directions, resulting in square elements. The air domain also contains a refinement, taking in account the effects of the jet flow and the surface elevation. The element size should then increase, progressively, between the mesh refinements regions and the outer boundaries of the model.

The mesh size of a computational model is usually one off the parameters that influences the most the results, being so important that it can even compromise the results applicability. Three meshes were produced and simulated, being their characteristics presented in Table 3. The results show that the mesh with smaller element size, 1.25mm, outputs smoother results. This element size is the one adopted for all the simulations, with the expense of an increased simulation time.

Table 3. Mesh characteristics, parametric study

Parameter	Model 1	Model 2	Model 3
Element Size	5mm	2.5mm	1.25mm
Fluid elements	4725	14490	49500
Structure elements	464	928	1856
FSI boundary elements	58	116	232
Mesh refinement factor	4	2	1
Computing time (h:min)*	0:04	0:19	1:17
Memory required	2.8 GB	8.2 GB	23.2 GB

* Using a 16-core, 3.4GHz workstation

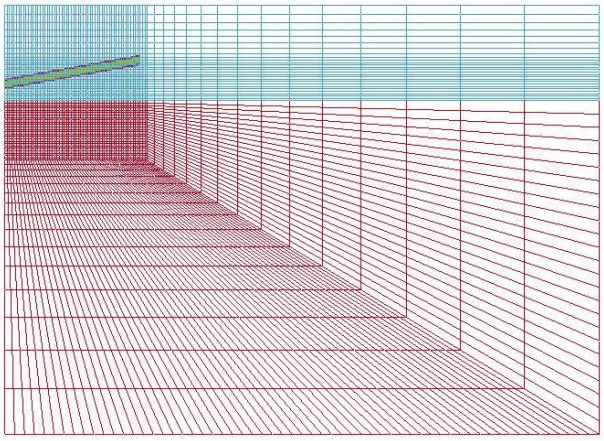

Figure 3. Computational model mesh.

3.5 *Boundary conditions and equations of state*

As the Eulerian fluid materials are defined as null, it's necessary to establish an equation of state for each of them. For the water, the Gruneisen equation of state is chosen, while in the case of the air, the linear polynomial equation of state was adopted, as explained in Wang and Guedes Soares (2014b)

To achieve two-dimensionality, the dimension of the model in the Z direction is only one element size.

It's also necessary to limit all the nodal displacement in the Z direction.. The symmetric boundary condition is applied on the symmetry plane wall of the model. Non-reflecting boundary conditions are also added to the other outer walls of the fluid domain, eliminating possible reflections. Velocity inputs are added to the keel point and to the other end of the wedge. Additionally, in the first time-step, an initial velocity is added to all nodes of the wedge, eliminating the initial vibrations of the wedge. The simulation time is calculated through the wedge geometry and the initial velocity to make sure that the section will be totally submerged in the water.

3.6 *Model setup*

The ALE method uses penalty forces to accomplish the coupling between the fluid and the structure. The penalty factor PFAC, is a scale parameter that acts on these penalty forces. LS-Dyna provides a specific output to quantify the energy absorbed by the coupling mechanism which is the contact energy output. The penalty factor should be tuned in a way that the contact energy absorbed at the coupling interface is small when compared to the internal energy, which is the energy contained in the system. It's possible for LS-Dyna to output a result with negative contact energy. This indicates that the model needs better parameter tuning and can also indicate other problems like leakage. Adopting a low PFAC value results in a very stiff structure which induces forces on the structure that are not real, as can be seen in the average pressure comparison example of Figure 4. These can be easily noticed with the increase of the contact energy, as demonstrated in the Figure 5 example. On the other hand, an higher PFAC value results in undesired oscillations in the fluid structure interface and can result in leakage. A good compromise for moderate deadrise and impact velocities is generally obtained by using 0.01 as the value for PFAC.

The number of coupling points parameter, NQUAD, determines how many points, equally divided, in each Lagrangian segment are dedicated to the coupling algorithm. During the simulation, the algorithm applies the coupling forces to these points. Similar to the PFAC, a higher number of coupling points increases simulation time but reduces leakage at the fluid structure interface. Three coupling points are generally sufficient to model the interface.

Finally, the time step factor enables the user to establish a scale coefficient in relation to the critical time step calculated by the software. Reducing the time step factor can help solving instability issues caused by the fast-evolving nature of the simulation but will also result in longer simulation times. Adopting 0.9 as the general value for the time step factor is generally sufficient.

As explained earlier, the setup parameters presented above are generally adequate for moderate velocities and deadrises, but each simulation must be checked in terms of stability and validity, as the lower deadrises and higher impact will often present problems like leakage or other instability issues.

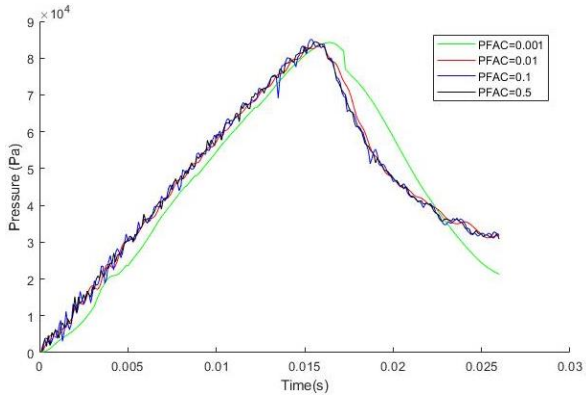

Figure 4. Average pressure comparison example.

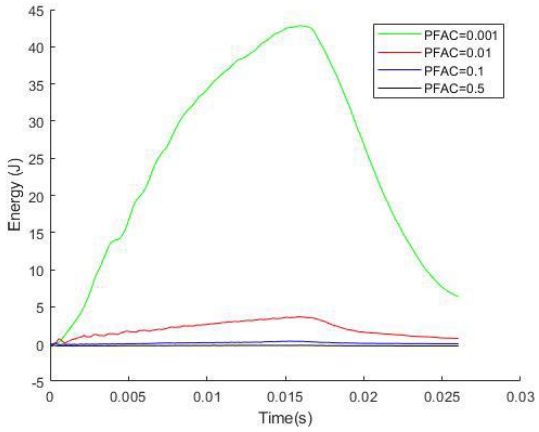

Figure 5. Contact energy comparison example.

4 RIGID BODY MODEL VALIDATION SETUP

Rigid body model validation will be performed by comparing the computational results with the experimental results obtained by Zhao et al. (1996) and by the numerical ones of Luo et al. (2011). Figure 6 presents the geometry adopted. Table 4 describes the input parameters used in this validation simulation, in which the velocity case is free falling. To model the free-falling behavior, the velocity profile presented by Luo et al. (2011) was implemented.

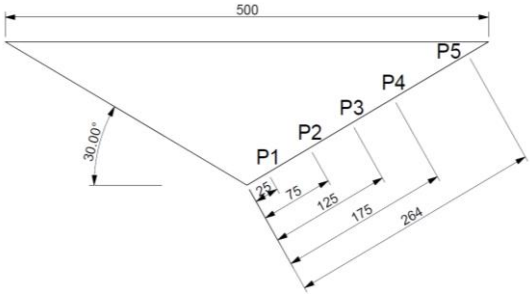

Figure 6. Geometry and gauge location of the experimental model adopted in Zhao's (1996) experiments.

Table 4. Setup parameters used in the rigid body simulation.

Velocity Model	Free-falling	
Initial Velocity	6.15	m/s
Deadrise	30	degrees
Mesh Size	1.25	mm
Penalty Factor	0.01	-
Time step factor	0.9	-
Number of coupling points	3	-
Simulation time	0.03	s

4.1 *Slamming force results comparison*

The slamming force result is presented and compared, in Figure 7, with Wagner (1932), Luo et al. (2011), Mei et al. (1999) and Zhao et al. (1996).

One should state that, during the simulations, the keel point only touches the surface of the water at the time instant of 0.0039s but, for the sake of simplicity, all the results presented will set this time instant to zero. The figure shows that the forces increase during the water entry, which then stabilize and abruptly drops. The slamming force drops greatly because of the flow separation which occurs when the water up-rise reaches the end of the wedge as illustrated in Figure 8. Figure 7 indicates that the results agree very well with each other, with only the Wagner´s results overestimating the force results. The differences presented to the results obtained by Luo et al. [13] can be explained by the fact that although the computational model is very similar, there is a small difference in the wedge length.

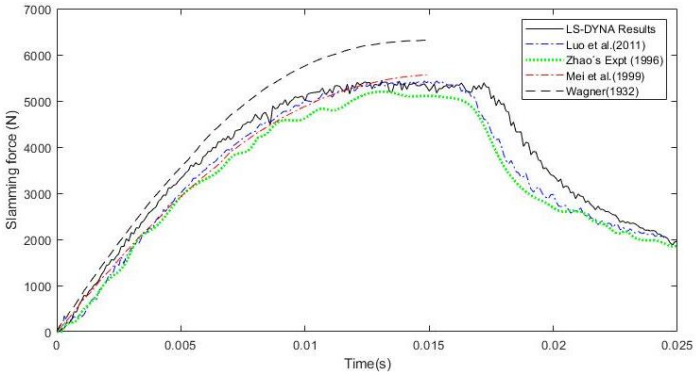

Figure 7. Slamming force time history comparison.

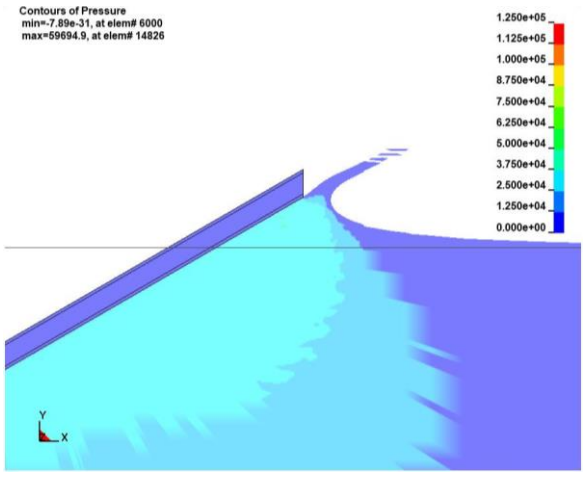

Figure 8. Water surface elevation and distribution of pressures.

4.2 *Pressure time history at given locations*

Zhao et al. (1996) included in their experimental model, five pressure sensors installed at the locations presented earlier in the Figure 6. Figure 9 presents the comparison between Zhao's results and the present results obtained in the LS-DYNA model.

The time histories show good similarity between each one of the results.

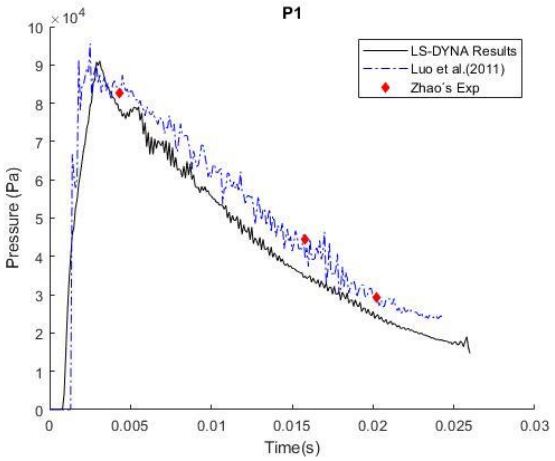

(a) Gauge P1

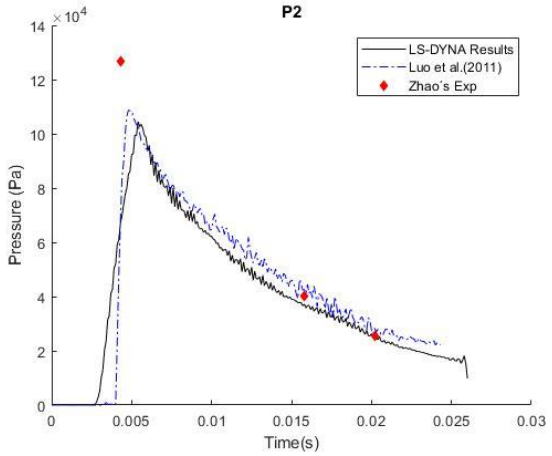

(b) Gauge P2

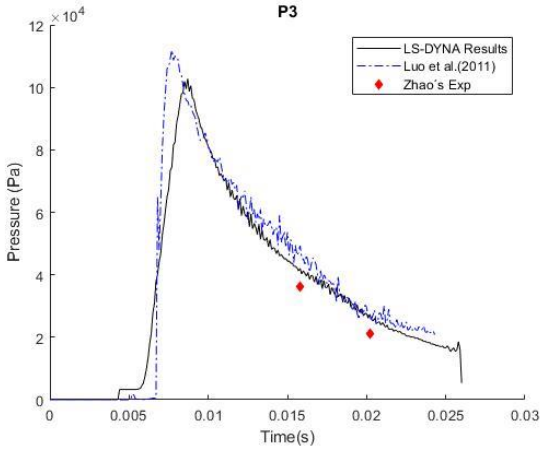

(c) Gauge P3

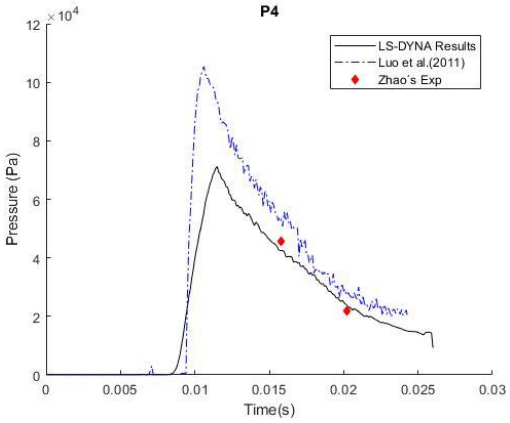

(d) Gauge P4

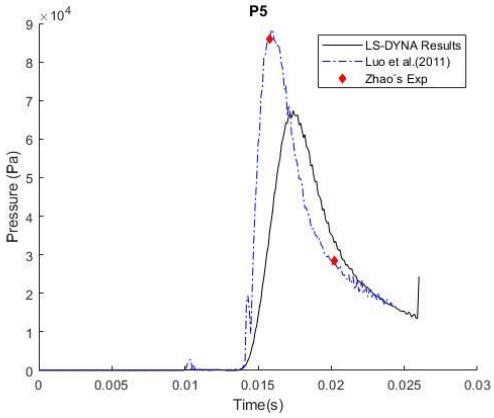

(e) Gauge P5

Figure 9. Pressure time history at different locations.

In the gauges P3 and P4, both numerical results show a slightly variation from Zhao's results, although the developed patterns are the same. In the case of P1 and P5 the results obtained in LS-DYNA are consistent with the experimental ones. In the pressure gauge P2, the results also show good agreement, although the predicted peak pressure by the numerical methods is lower than the one obtained in experiments, which can be caused if the mesh is note fine enough to capture the peak value or if the capturing frequency is not high enough.

4.3 *Pressure coefficient*

The maximum slamming pressures on the rigid wedges with β=10º, 20º and 30º are calculated using equation (4) and based on the simulation results. The results are presented in Figure 10, which also includes the numerical results obtained by Luo et al. (2011), the analytical results which can be obtained by the Wagner (1932) formulation, and the results from Ochi and Motter (1973) and Stavovy and Chuang (1976) empirical formulations. The results show that all the methods show good agreement with each other when the deadrise is large. However, the small deadrise angles leads to big differences in the results. This is somehow expected, since the small deadrises are often harder to numerically simulate due to the fast-evolving nature of the problem.

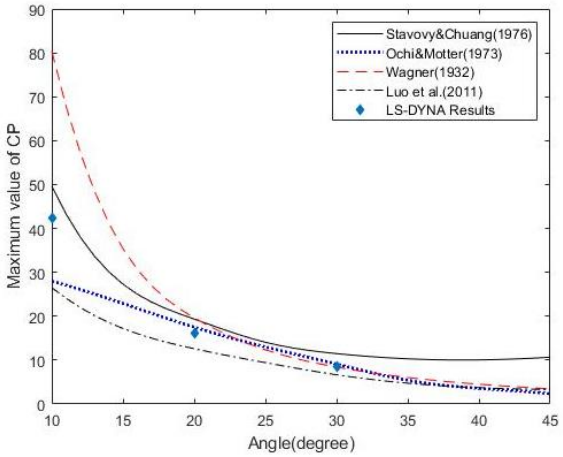

Figure 10. Variation of the maximum pressure coefficient with the deadrise.

5 COMPOSITE BODY MODEL VALIDATION

A model validation was performed based on the experiments proposed by Hasson et al. (2017). This validation now includes hydroelasticity which requires the structure to be flexible.

5.1 *Composite body model validation setup*

In order to proceed with the validation, the model was built using the same geometry, materials and loadings as the ones present by Hasson et al. (2017). The geometry, which is presented in Figure 11, is composed by two sandwich plates fixed at both ends and at the keel. The length of each plate is 500mm and the deadrise is fixed for all the experiments at 10º. The two sandwich plates were composed by two FRP skins with a thickness of 7mm each and a 20mm PVC foam core. Additionally, each plate has a width of 250mm. In this numerical study, only a two-dimensional problem is simulated, but the width must be taken in account when comparing dimensional results like the slamming forces. The experiments included three strain gauges installed at the locations demonstrated in the same figure.

The computational model parameters are presented in Table 5. In this case, the velocity profile presented in Hasson et al. (2017) is used. By defining that t=0 means the moment when the keel touches the water surface, an initial velocity of 6.0m/s is obtained. The initial simulation presented leakage at the fluid structure interface, due to the nature of the problem, being it corrected by modifying NQUAD and PFAC.

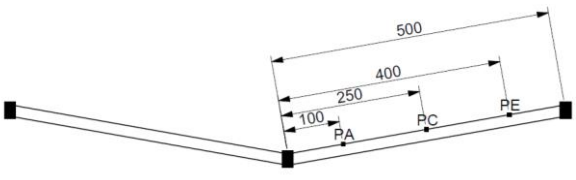

Figure 11. Experimental model adopted by Hasson et al. [16].

Table 5. Setup parameters used in the composite body simulation.

Velocity Model	Variable	
Initial Velocity	6.0	m/s
Deadrise	10	degrees
Mesh Size	1.25	mm
Penalty Factor	0.005	-
Time step factor	0.4	-
Number of coupling points	5	-
Simulation time	0.022	s

5.2 *Slamming force comparison*

The slamming force results presented in Figure 12 show good agreement with each other. Both computational models show higher peak force when compared with the experimental result, this can be caused, for instance, by the effect of the third-dimension present in the experiments.

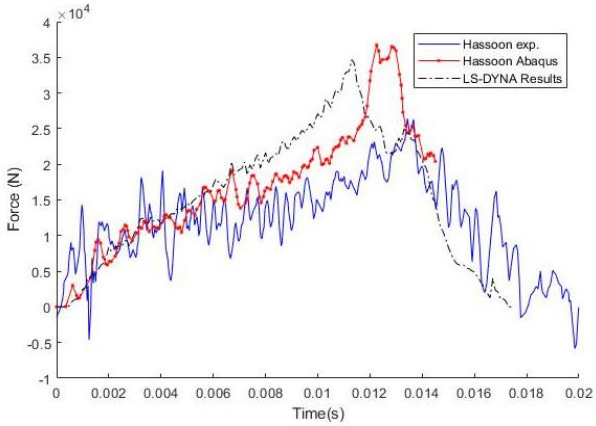

Figure 12. Vertical slamming force comparison.

5.3 *Structure strain comparison*

The strain results comparison between the experimental and the numerical results obtained in LS-Dyna are presented in Figure 13. The results obtained in the experiments tend to present themselves earlier during the time history and hold their value longer. The strain gauges calibration is a possible cause, but the overall comparison shows very good correlation.

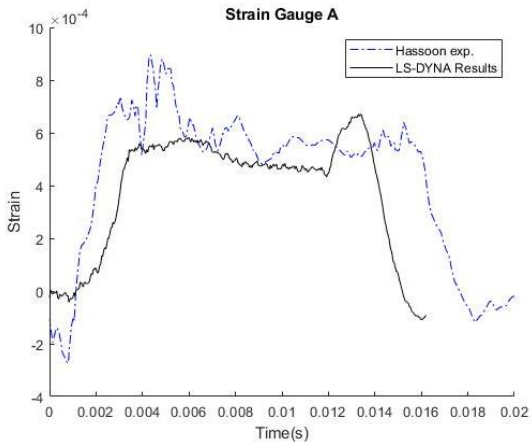

(a) Strain gauge A

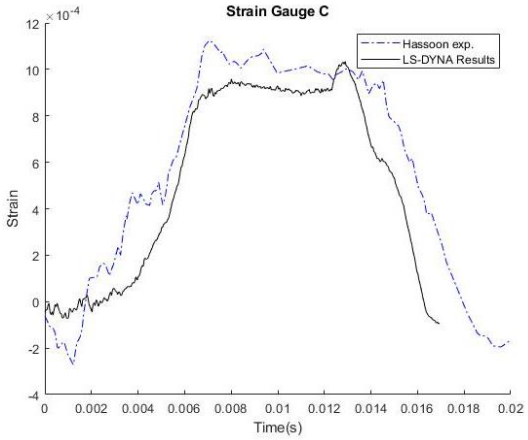

(b) Strain gauge C

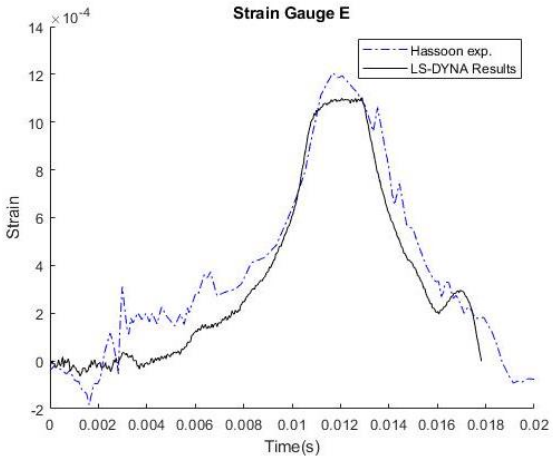

(c) Strain gauge E

Figure 13. Structure strain results comparison.

6 HYDROELASTICITY STUDY

The hydroelasticity effect in the water entry of wedges is studied through the comparison of the results obtained for the rigid composite wedge with the ones obtained for the flexible composite wedge.

The simulations setup parameters are presented in the Table 6. To eliminate any possible pressure difference caused by differences in the velocity between the rigid and the flexible case, the velocity is constant and equal to initial velocity of the case. Due to the different deadrises and velocities, it is necessary to increase the number of coupling points, NQUAD, in the simulations with lower deadrise.

Table 6. Setup parameters used in the hydroelasticity simulation.

Velocity model	Constant	
Initial velocity	4 / 6 / 8 / 10	m/s
Deadrise	10 / 20 / 30	degrees
Mesh size	1.25	mm
Penalty factor	0.01	-
Time step factor	0.4	-
Number of coupling points	Between 3 and 5	-

6.1 *Hydroelasticity effect comparison*

The comparison of the pressure coefficient between the rigid and the flexible body for the three deadrise cases with a fixed drop velocity of 4 and 10 m/s are presented in Figure 14.

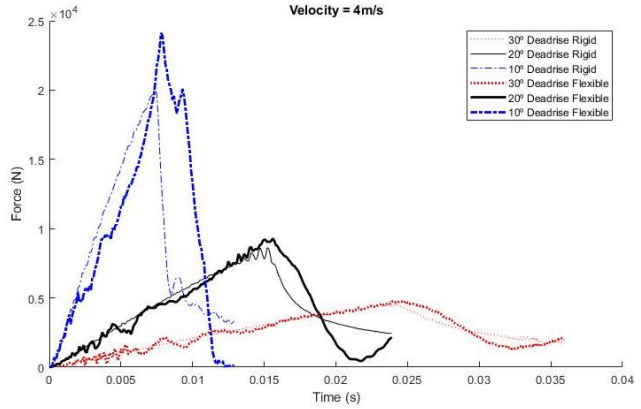

(a) 4m/s Drop Velocity

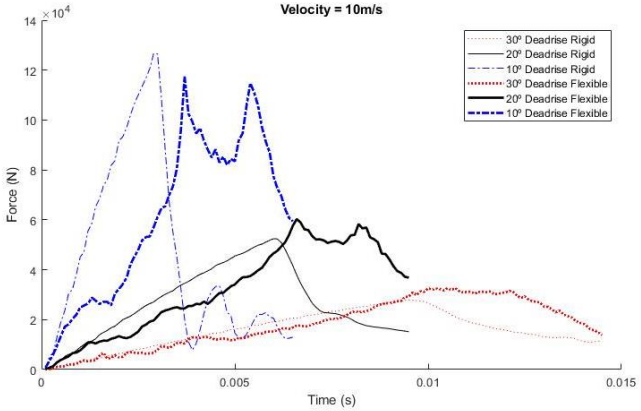

(b) 10m/s Drop Velocity

Figure 14. Hydroelasticity effect comparison, average forces.

The results indicate that in the high deadrise, low velocity cases, the pressure rises similarly in both the rigid and flexible cases, but the flexible body will present a higher peak pressure. This is to be expected due to the fact that, in the flexible composite body, the wedge displacement will result in a smaller local deadrise which then results in higher pressures. The high velocity, low deadrise cases show that in the first stages of the impact, the pressure result observed in the flexible body is lower than the rigid body, but then the flexible body holds a higher pressure longer. This can be explained by the elastic behavior of the body, in which the impact is firstly dampened by the body elasticity which then presents its peak value later. The second pressure peak occurs due to the extreme wedge displacement, which induces a pressure accumulation below the wedge. In these cases, the pressure peak occurring when the water reaches the wedge end, start to travel backwards towards the keel, where it will present its peak value again. This behavior can also be observed in the pressure distribution comparison of Figure 15, which corresponds to extreme case of the 10º deadrise, 10m/s drop velocity, at the location P2 of the wedge.

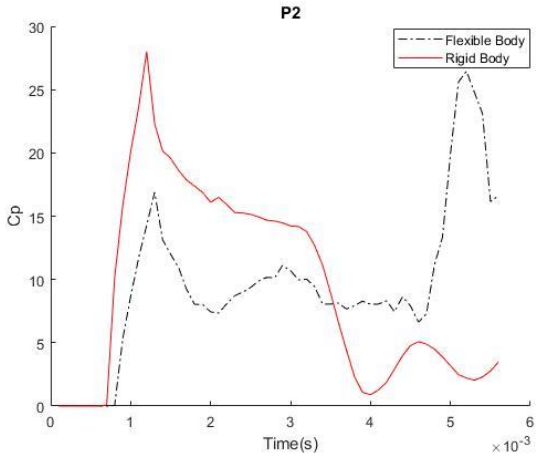

Figure 15: Pressure distribution comparison at the given location P2, 10º deadrise, 10m/s drop velocity case.

6.2 *Forces and displacements*

Figure 16 and Figure 17 present the forces and displacements for the 10º deadrise flexible composite case.

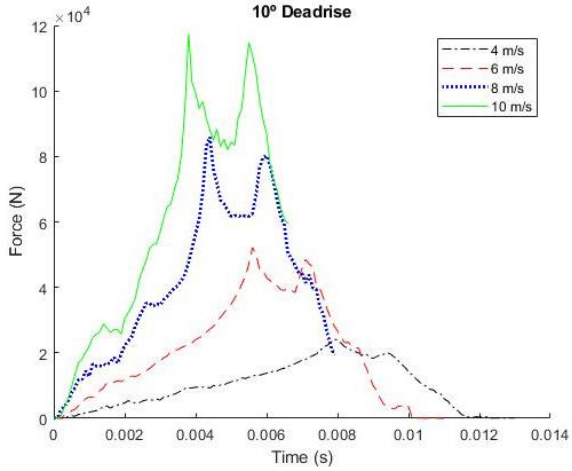

Figure 16: Force comparison, 10º deadrise flexible composite wedge.

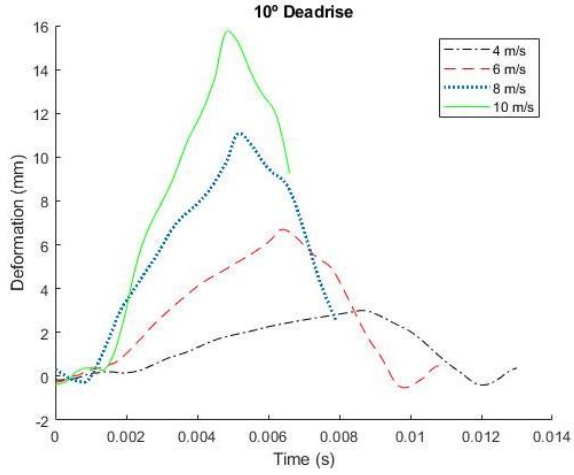

Figure 17: Displacement comparison, 10º deadrise flexible composite wedge.

The results show good agreement between each other as the slamming forces peeks can be observed in the middle point displacement curves. The second peak effect observed and explained earlier can, once again, be observed in the high velocity displacement curves, as the rate of descent after the peak value of these curves is not constant.

7 CONCLUSIONS

The water entry of two-dimensional composite wedges was simulated using the LS-DYNA commercial code which is equipped with an Arbitrary Lagrangian Eulerian (ALE) solver.

The composite structure was fully modeled in solid elements, which is advantageous if the user is interested in the out of plane stress/strain results. This requires the composite material properties in the out of plane direction, which in this case, were retrieved from the Bureau Veritas rules for the classification of composite vessels. These properties are a good guideline for the design of marine structures with composites, however, since the composite materials are very sensitive, one should not take them for granted. Proper material testing must always be performed.

The 30º deadrise angle rigid wedge, free drop case, was carried in order to validate fluid part of the model. The comparison with the other available numerical, experimental and analytical indicated good agreement between the results, with a small difference in the pressure peak value, which can be caused by three-dimensional effects in the experiments.

On the other hand, the simulation of the flexible composite wedge with 10º deadrise angle has good agreement with the experimental data. Small differences were observed in the peak values of the slamming forces but the difference in dimensionality is also present.

The comparison between the rigid and the flexible composite wedge show that the hydroelasticity is an effect that must certainly induce additional loads on the structure, especially when the structure has a low stiffness, since the bigger the displacement the higher are the additional pressure loads caused by the structural displacements.

REFERENCES

Aquelet, N., Souli, M. and Olovsson, L. (2006). Euler-Lagrange coupling with damping effects: Application to slamming problems. *Computer Methods in Applied Mechanics and Engineering. Vol. 195, pp. 110-132.*

Bureau Veritas (2012). Hull in Composite Materials and Plywood, Material Approval, Design Principles, Construction and Survey. *NR 546 DT R00 E.*

Faltinsen, O.M. (1999). Water entry of a wedge by hydroelastic orthotropic plate theory. *Journal of Ship Research.* Vol.3, pp 180-193.

Hassoon, O.H., Tarfaoui, M., El Malk Alaoui, A., El Moumen, A. (2017). Experimental and numerical investigation on the dynamic response of sandwich composite panels under hydrodynamic slamming loads. *Composite Structures.* Vol. 178, pp 297-307.

Lu, C.H., He, Y.S., Wu, G.X., 2000. Coupled analysis of nonlinear interaction between fluid and structure during impact. Journal of Fluid and Structures, 14, 127-146.

Luo, H., Wang, S., Guedes Soares, C. (2011). Numerical prediction of slamming loads on a rigid wedge subjected to water entry using an explicit finite element method. *Advances in Marine Structures,* pp. 41-48.

Mei, X.M., Liu, Y.M. and Dick, K.P. (1999). On the water impact of general two-dimensional sections. *Applied Ocean Research. Vol. 21,* pp. 1-15.

Ochi, M.K. and Motter, L.E. (1973). Prediction of slamming characteristics and hull response for ship design, *Transactions SNAME. Vol. 81, pp.* 144-190.

Qin, Z. and Batra, R.C., 2009. Local slamming impact of sandwich composite hulls. *International Journal of Solids and Structures*, 46(10), pp.2011-2035.

Santos, F. M., Temarel, P. A., Guedes Soares, C., 2009. On the Limitations of Two and Three-dimensional Linear Hydroelasticity Analyses Applied to a Fast Patrol Boat. *Journal of Engineering for the Maritime Environment*. 223(3), 457-478.

Stavovy, A.B. and Chuang, S.L. (1976). Analytical determination of slamming pressures for high speed vessels in waves, *Journal of Ship Research. Vol. 20,* pp. 190-198.

Wagner, H. (1932) Uber Stossund Gleitvergange an der Oberflache von Flussigkeiten. *Zeitschrift fuer Angewandte Mathematik und Mechanik.* Vol. 12, pp. 193–215.

Wang, S. and Soares, C.G., 2017. Review of ship slamming loads and responses. *Journal of Marine Science and Application, 16(4),* pp.427-445.

Wang, S., Guedes Soares, C., 2014a. Comparison of simplified approaches and numerical tools to predict the loads on bottom slamming of marine. *Developments in Maritime Transportation and Exploitation of Sea Resources*, Guedes Soares, C. and López Peña F. (Eds.). Francis & Taylor Group, London, UK, pp. 157-170.

Wang, S., Guedes Soares, C., 2014b. Numerical study on the water impact of 3D bodies by explicit finite element method. *Ocean Engineering* 78:73–88.

Wang, S., 2011. Assessment of slam induced loads on two dimensional wedges and ship sections. Master thesis. Portugal: University of Lisbon.

Wang, S., Karmakar, D. and Soares, C.G., 2016. Hydroelastic impact of a horizontal floating plate with forward speed. *Journal of Fluids and Structures*, 60, pp.97-113.

Wang, S. and Guedes Soares, C., 2012. Analysis of the water impact of symmetric wedges with a multi-material Eulerian formulation. *International Journal of Maritime Engineering,* 154(10), pp.191-205.